RMJG Rutile: A New Natural Reference Material for Microbeam U-Pb Dating and Hf Isotopic Analysis

Le **Zhang** (1)* (iD), Jia-Lin **Wu** (2), Jia-Run **Tu** (3), Dan **Wu** (4), Nan **Li** (5), Xiao-Ping **Xia** (1) (iD) and Zhong-Yuan **Ren** (1)

(1) State Key Laboratory of Isotope Geochemistry, Guangzhou Institute of Geochemistry, Chinese Academy of Sciences, Guangzhou, 510640, China
(2) School of Earth Science and Resources, Chang'an University, Xi'an, 710054, China
(3) Tianjin Centre, China Geological Survey, Tianjin, 300170, China
(4) Key Laboratory of Mineralogy and Metallogeny, Guangzhou Institute of Geochemistry, Chinese Academy of Sciences, Guangzhou, 510640, China
(5) Guangdong Key Laboratory of Integrated Agro-environmental Pollution Control and Management, Guangdong Institute of Eco-environmental Science and Technology, Guangzhou, 510650, China
* Corresponding author. e-mail: zhangle@gig.ac.cn

Matrix-matched reference materials are necessary for accurate microbeam U-Pb dating and Hf isotopic determination. This study introduces the RMJG rutile as a new potential reference material, which was separated from Palaeoproterozoic pelitic granulites collected in Hebei Province, China. LA-ICP-MS measurements indicate the RMJG rutile has extremely low Th (< 0.003 ± 0.01 µg g^{-1}) and common Pb contents, but high Hf (102 ± 34 µg g^{-1}), U (61 ± 11 µg g^{-1}), and radiogenic Pb (~ 20 µg g^{-1}) contents. Moreover, the rutile yields relatively constant U-Pb ages and Hf isotopic data. The LA-ICP-MS analyses suggest that this rutile has a concordant U-Pb age with a statistical mean ^{206}Pb/^{238}U and ^{207}Pb/^{235}U ages of 1749.9 ± 32.1 Ma and 1750.0 ± 26.4 Ma, respectively (2s), which are statistically indistinguishable from its ID-TIMS ages (1750.6 ± 8.4 and 1750.1 ± 4.7 Ma). Precise determination of the ^{176}Hf/^{177}Hf ratio by MC-ICP-MS in solution mode (0.281652 ± 0.000006) is in good agreement with the statistical mean of the LA-MC-ICP-MS measurements (0.28166 ± 0.00018). Therefore, the limited variations of RMJG U-Pb age and Hf isotopic composition together with its extremely low common Pb and high Hf, U and Pb contents make it an ideal calibration and monitor reference material for LA-ICP-MS measurements.

Keywords: RMJG rutile, U-Pb geochronology, ID-TIMS, LA-ICP-MS, reference material.

Rutile (TiO$_2$) is a widely distributed accessory mineral in moderate- to high-pressure metamorphic rocks and in sedimentary rocks. Rare magmatic rocks (e.g., anorthosites, pegmatites and quartz veins) also contain this mineral. Rutile attracts much attention from the Earth Science community (Meinhold 2010, Triebold *et al.* 2012, Zack and Kooijman 2017) due to its: (a) significant U content, low common Pb content and resistance to weathering, which makes rutile an important geochronometer (Mezger *et al.* 1991, Luvizotto *et al.* 2009, Kooijman *et al.* 2010, Li *et al.* 2011, Zack *et al.* 2011, Xia *et al.* 2013, Axelsson *et al.* 2018); (b) temperature-sensitive Zr content, which allows rutile to be used as a geothermometer in metamorphic rocks (Zack *et al.* 2004a, Watson *et al.* 2006, Zack and Luvizottow 2006, Tomkins

et al. 2007, Zheng *et al.* 2011, Ewing *et al.* 2013, Pape *et al.* 2016); (c) Cr-Nb-Zr contents, which provide an indication of the source lithology (Zack *et al.* 2004b, Stendal *et al.* 2006, Meinhold *et al.* 2008, Triebold *et al.* 2012); and (d) moderate Hf content (~ 50 µg g^{-1}) that allows Hf isotopic measurement of rutile by LA-MC-ICP-MS to trace heterogeneous sources (Ewing *et al.* 2011, 2014, Li *et al.* 2015a).

Irrespective of the analytical technique, matrix-matched reference materials are required for accurate microbeam U-Pb age and Hf isotopic measurements. At present, reported rutile reference materials include R10, R19 (Luvizotto *et al.* 2009, Zack *et al.* 2011), Sugluk-4 and PCA-S207 (Bracciali

et al. 2013) and R632 (Axelsson *et al.* 2018). The Hf contents (38–51 µg g^{-1}; Li *et al.* 2015a) of these rutiles are not high enough to serve as reference materials for microbeam Hf isotopic determination. As such, the application of microbeam rutile U-Pb dating and Hf isotopic studies is limited by the lack of suitable reference materials. In this study, we report microbeam U-Pb age and Hf isotopic data for RMJG rutile crystals, which are hosted in Palaeoproterozoic pelitic granulites from Hebei Province, China. Our data suggest that the RMJG rutile can be used as a new reference material for microbeam determination of U-Pb ages and Hf isotopes in rutile.

Geological background and sample description

The pelitic granulite hosting the RMJG rutile is part of the Huai'an complex, which is located in the north-central part of the North China Craton (Figure 1a). The Huai'an complex comprises six lithological units from northwest to southeast, including the Shuigoukou grey gneisses, HP mafic granulites, the Khondalite Series, Dongjiagou granitic gneiss and Dapinggou garnet-bearing granite (Figure 1b; see Wu *et al.* 2016 for detailed descriptions). The Shuigoukou grey gneisses underwent multi-stage deformation and high-grade metamorphism; geochronological data indicate that the Shuigoukou gneisses and the banded gneisses were emplaced before 2.44–2.50 Ga. The metamorphic peak conditions of the HP mafic granulites and Khondalite Series rocks was suggested at 11–15 kbar, 750–880 °C. The Khondalite Series rocks were considered to be metamorphosed at middle-pressure granulite facies. Both types of granulite terranes have similar metamorphic ages of about 1.95–1.80 Ga. The Dongjiagou granitic gneiss and Dapinggou garnet-bearing granite were emplaced at about 2.04 and 1.85 Ga, respectively. Detailed descriptions of the field geology and petrography can be found in Wu *et al.* (2016, 2018, 2019). Zircon U-Pb dating of the Manjinggou pelitic granulite has yielded two distinct age populations of 1916 ± 30 and 1840 ± 24 Ma, interpreted to represent the time of high-pressure granulite-facies metamorphism and intermediate- to low-pressure granulite-facies metamorphism, respectively (Wu *et al.* 2019).

The sampled outcrop is *ca.* 50 km to the southeast of Huai'an County (114°28.5'E, 40°22.99'N). The exact sampling position is around the location of sample MJG3 in Wu *et al.* (2016) (Figure S1). The pelitic granulite hosting RMJG rutile is a coarse-grained garnet–sillimanite–K-feldspar gneiss, with a mineral assemblage of quartz, garnet, K-feldspar, sillimanite, biotite, kyanite, plagioclase, muscovite and minor rutile, spinel, ilmenite, graphite, pyrite and pyrrhotite. The pelitic granulite was crushed by High-Voltage Pulse Fragmentor (SelFrag, Kerzers, Switzerland), which minimised the destruction of mineral grains. Most RMJG rutiles are euhedral, 200–300 µm in length, translucent and brown–red to dark brown in colour with length-to-width ratios of 1:2 to 1:3 (Figure 2a). Fractures and small inclusions are visible in some rutile grains. No zoning was observed in back-scattered electron images (Figure 2b).
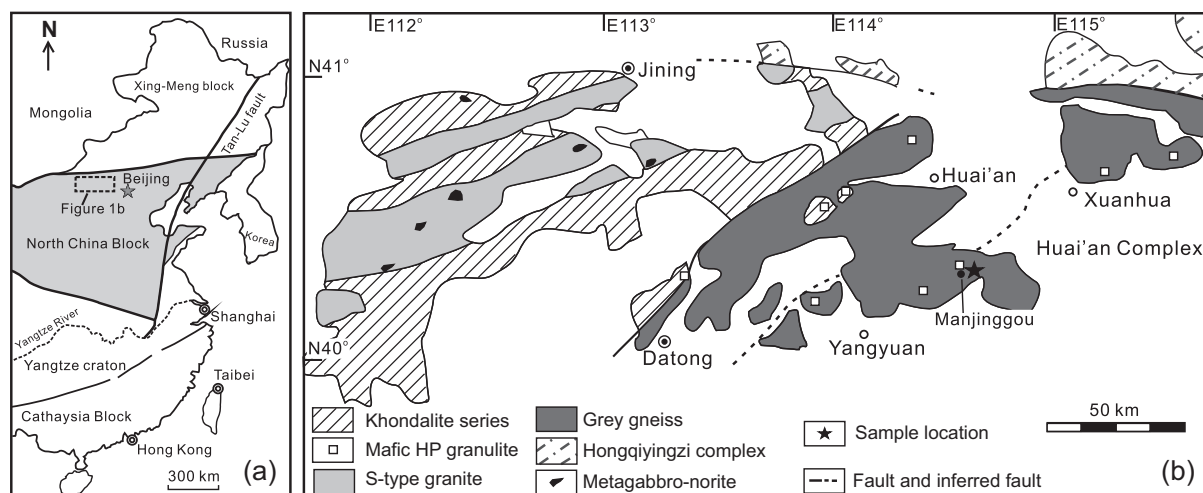

Figure 1. (a) Simplified tectonic map of east China. (b) Regional geological map showing the sampling location of the RMJG rutile, after Zhai *et al.* (2003).
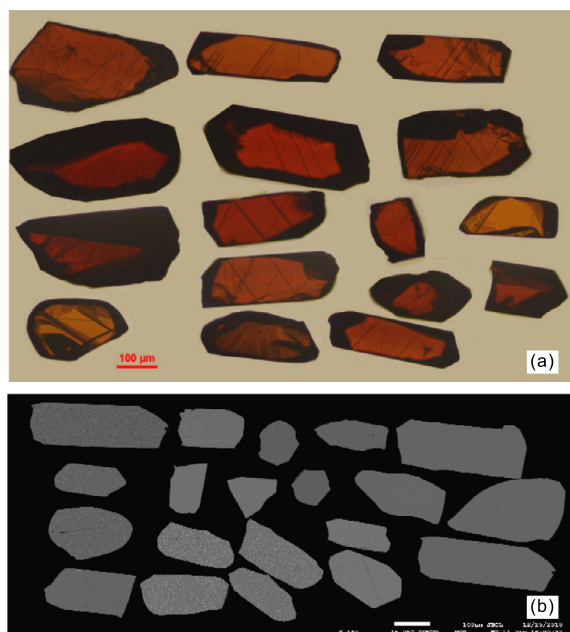
Figure 2. (a) Image of the RMJG rutile grains. (b) BSE image of the RMG rutile grains. Both scale bars are 100 μm. [Colour figure can be viewed at wileyonlinelibrary.com]

Analytical methods

High-resolution X-ray elemental mapping

High-resolution X-ray elemental mapping for Zr, Nb, Cr, Hf and U was carried out using a JEOL JXA-8230 electron microprobe at the Key Laboratory of Mineralogy and Metallogeny (KLMM) in Guangzhou Institute of Geochemistry (GIG), Chinese Academy of Sciences (CAS). The electron microprobe was operated at an accelerating voltage of 20 kV, a probe current of 300 nA and a beam size of 1 μm (Xing *et al.* 2017). Hafnium Lα, Cr Kα and V Kα X-rays were analysed using a LIF crystal. Niobium Lα X-rays were analysed using a PET crystal. Uranium Mα and Zr Lα X-rays were analysed with a PETH crystal. The step size was 1 μm, and the dwell time was set to 100 ms for each point.

LA-ICP-MS trace element determination

Trace element contents of the RMJG rutiles were measured with a Thermo Fisher ELEMENT XR sector-field ICP-MS, which was coupled to a RESOlution-M 50 laser ablation system, at the State Key Laboratory of Isotope Geochemistry (SKLIG), GIG-CAS. The laser was operated at a beam size of 24 μm, repetition rate of 6 Hz and energy density of 4 J cm^{-2}. Each analysis consisted of 20 s of gas blank collection with the laser off and 30 s of sample signal collection with the laser on. Ion beam intensities on masses ^{45}Sc, ^{49}Ti, ^{51}V, ^{52}Cr, ^{66}Zn, ^{91}Zr, ^{93}Nb, ^{178}Hf, ^{181}Ta, ^{232}Th and ^{238}U were measured in peak jumping mode. The torch shield was switched off to reduce the oxide production (^{16}O^{238}U/^{238}U) to < 0.3% (Kimura and Chang 2012, Zhang *et al.* 2019). Trace element contents were determined by a multi-reference material calibration method, with the USGS glasses BCR-2G, BHVO-2G and Gs-1G used as reference materials. Details of data reduction procedures employed are described in Zhang *et al.* (2019). Two MPI–DING reference glasses (ATHO-G and ML3B-G) were used as monitor reference materials. The results for the MPI–DING glasses indicate that all the measured elemental contents agree within 5–8% of their preferred values.

ID-TIMS U-Pb dating

ID-TIMS U-Pb dating of the RMJG rutiles was conducted at the Tianjin Centre, China Geological Survey. Rutile crystals were handpicked under a microscope to avoid grains with inclusions or fractures. A chemical pre-treatment procedure was carried out in an ultraclean laboratory. All acids used were purified three times by sub-boiling distillation (Savillex Corporation, Minnetonka, MN, USA), and ultrapure water was produced from a Milli-Q system. Sample washing, digestion and U-Pb purification procedures were based on Tu *et al.* (2016) and Zhou *et al.* (2013). Approximately 14 mg of selected rutile grains were successively soaked in ultrapure anhydrous alcohol, 7 mol l^{-1} HNO$_3$ and 2 mol l^{-1} HCl for 3, 4 and 12 h, respectively, in order to remove any surface contamination. The HNO$_3$ and HCl leaching were undertaken on a hot plate at 80 °C. The sample grains were then divided into eight aliquots, and each was treated as an independent sample. Rutile grains were then crushed in a clean agate mortar and pestle to powders of ∼ 200 mesh. Sample powders were successively soaked in ultrapure anhydrous alcohol, 7 mol l^{-1} HNO$_3$ and 2 mol l^{-1} HCl for 3, 4 and 12 h, respectively, to negate the influence of small fractures or inclusions. Approximately 1–2 mg samples were weighed accurately and placed into acid-cleaned 10 ml PTFE beakers. Subsequently, 2 ml of concentrated HCl was added to the rutile, which resulted in complete digestion after 72 h in a temperature-controlled oven at 195 °C. The digested sample solutions were divided into two aliquots. One was used for Pb isotopic ratio measurements (*ca.* 70%), and the other was used for measuring the U-Pb contents (*ca.* 30%) to which four drops (*ca.* 30 mg) of a mixed ^{208}Pb-^{235}U spike was added. These solution aliquots were weighed accurately and then evaporated to dryness on a hot plate at 125 °C, and subsequently dissolved in 1 ml of a solution that contained two parts 2 mol l^{-1} HCl and one part 1 mol l^{-1} HBr. Lead

and U were separated using AG1 × 8 anion exchange resin. The purified Pb and U fractions were loaded with H_3PO_4 and silica gel onto degassed Re single filaments, respectively, and then dried at low temperature. U-Pb isotopic ratios were measured on a Triton TIMS (Thermo Fisher, Bremen, Germany). Lead isotopic ratios were measured at a temperature of 1250–1400 °C, while U isotopic ratios were measured at a temperature of 1350–1500 °C. Total procedural blanks during this study were 50 and 18 pg for Pb and U, respectively. Instrumental mass bias was corrected using the reference samples U500 and NBS 982. The data were processed using PBDAT (Ludwig 1988) and Isoplot (Ludwig 2005) software. Common Pb was monitored using ^{204}Pb, and corrections were made based on the blank Pb isotopic composition and initial Pb isotopic composition given by the model of Stacey and Kramers (1975).

LA-MC-ICP-MS, LA-SF-ICP-MS and LA-ICP-MS U-Pb dating

Microanalysis of U-Pb dating of the RMJG rutiles was conducted using LA-MC-ICP-MS, LA-SF-ICP-MS and LA-ICP-MS in SKLIG and KLMM, GIG-CAS. The analytical procedures for LA-MC-ICP-MS are similar to those described in Xia *et al.* (2013) and are summarized in Table S1. A RESOlution M-50 (Resonetics, Nashua, NH, USA) 193 nm laser ablation system was connected to a Neptune Plus (Thermo Fisher) MC-ICP-MS. ^{202}Hg, $^{204}(Hg + Pb)$, ^{206}Pb, ^{207}Pb, ^{208}Pb, ^{232}Th and ^{238}U were simultaneously detected with seven ion counters in static mode. The ^{202}Hg signal was used to correct for the isobaric interference of ^{204}Hg on ^{204}Pb during ablation. Before each spot analysis, five laser shots were used to remove any contamination on the rutile surface. Each spot analysis comprised 25 s of gas blank collection with the laser off and 30 s of sample signal collection with the laser on. The laser was operated at a beam size of 24 μm, repetition rate of 5 Hz and energy density of 4 J cm^{-2}. Common Pb was corrected by using the measured non-radiogenic ^{204}Pb with the Pb evolution model of Stacey and Kramers (1975). All rutile grains analysed by LA-MC-ICP-MS showed negligible ^{204}Pb ($^{206}Pb/^{204}Pb > 2000$).

Microbeam U-Pb dating by LA-SF-ICP-MS was performed with the same laser ablation system (RESOlution-M 50) and mass spectrometer (ELEMENT XR ICP-MS) used for trace element determination at SKLIG-GIG. The laser was operated at a beam size of 33 μm, repetition rate of 5 Hz and energy density of 4 J cm^{-2}. Each analysis consisted of 30 s of gas blank collection with the laser off and 30 s of sample signal collection with the laser on. Signals on masses ^{202}Hg, $^{204}(Hg + Pb)$, ^{206}Pb, ^{207}Pb, ^{208}Pb, ^{232}Th and ^{238}U were detected in peak jumping mode with the torch shield

off. The mass window and sampling peak number for all the masses were set to 10% and 60, respectively. ^{202}Hg was used to calculate the interference of ^{204}Hg on ^{204}Pb. The resultant ^{204}Pb signal was used to correct for common Pb, although all rutile grains measured by LA-SF-ICP-MS contained negligible ^{204}Pb ($^{206}Pb/^{204}Pb > 2000$).

Microbeam U-Pb dating by LA-ICP-MS was conducted with a RESOlution S-155 (Resonetics) 193 nm laser ablation system connected to an Agilent 7900 (Japan) quadrupole ICP-MS. Each spot analysis incorporated ~ 30 s of background acquisition with the laser off and 40 s of sample data acquisition with the laser on. Dwell times were 5 ms for ^{206}Pb, ^{207}Pb and ^{238}U and 25 ms for ^{232}Th and ^{208}Pb. The laser was operated at a beam size of 32 μm, repetition rate of 5 Hz and energy density of 5 J cm^{-2}. Common lead was corrected for by assuming the ^{208}Pb signal intensity was non-radiogenic, given that rutiles have sufficiently low Th contents (Zack *et al.* 2011). The LA-MC-ICP-MS, LA-SF-ICP-MS and LA-ICP-MS methods all used the rutile reference materials R10 (1090 ± 5 Ma; Luvizotto *et al.* 2009) as the calibration material and R19 (489.5 ± 0.9 Ma; Zack *et al.* 2011) as the second reference material to evaluate the analytical precision and accuracy. All U-Pb ages were calculated with the Isoplot 3.22 program (Ludwig 2005). Errors on single spot analyses are expressed as ± 2s. Forty-four analyses of R19 by LA-MC-ICP-MS, thirty-four analyses by LA-SF-ICP-MS and thirty-eight analyses by LA-ICP-MS yielded mean $^{206}Pb/^{238}U$ ages of 487.8 ± 5.0 Ma (2s), 486.3 ± 5.9 Ma (2s) and 488.0 ± 6.8 Ma (2s), respectively, which agree well with its recommended value within analytical error.

Hf isotopic determinations

All Hf isotope determinations of RMJG rutiles were conducted on a Neptune Plus MC-ICP-MS, the same instrument as used for U-Pb dating, at SKLIG-GIG-CAS.

Solution MC-ICP-MS analysis

Rutile grains without cracks and inclusions were selected for analysis. The selected grains were crushed in an agate mortar to powders of ~ 200 mesh. Four duplicate rutile powders (each of *ca.* 5 mg) were digested in concentrated HF and HNO_3 (1:1 by volume) at 190 °C for 5 days. After evaporation, the samples were re-dissolved in 2 mol l^{-1} HCl and then evaporated again. The samples were then re-dissolved in 5 ml of 6 mol l^{-1} HCl for chemical separation on Ln resin. Most matrix and rare earth elements (REE) were eluted with 6 mol l^{-1} HCl. Titanium was eluted with 4 mol l^{-1} HCl + 0.5% H_2O_2. Hafnium was eluted with 2 mol l^{-1} HF

and then evaporated. Prior to MC-ICP-MS measurement, Hf was dissolved in 1.5 ml of 2% HNO_3. Nine Faraday collectors were used to measure ^{171}Yb, ^{173}Yb, $^{174}(Yb + Hf)$, ^{175}Lu, $^{176}(Yb + Lu + Hf)$, ^{177}Hf, ^{178}Hf, ^{179}Hf and ^{180}Hf simultaneously in static mode. The integration time was set to ~ 4 s. Instrumental mass bias was corrected based on the measured $^{179}Hf/^{177}Hf$ ratio and its natural ratio (0.7325; Blichert-Toft et al. 1997), using an exponential law. During the Hf isotopic measurements, six analyses of JMC14374 yielded a mean $^{176}Hf/^{177}Hf$ value of 0.282191 ± 0.000005 (2s), consistent with the recommended value (0.282189 ± 0.000019) of Wu et al. (2006).

LA-MC-ICP-MS analysis

The same laser ablation system (RESOlution M-50) used for U-Pb dating was utilised for microbeam Hf isotopic determination. Each analysis comprised 25 s of gas blank collection with the laser off and 40 s of sample signal collection with the laser on. The laser was operated at a beam size of 155 μm, repetition rate of 8 Hz and energy density of 4 J cm^{-2}. The collector array was the same as that used for solution analysis. The integration time was set to 0.131 s. To improve the instrumental sensitivity, Jet sample and X skimmer cones were used at the interface (Hu et al. 2012, Zhang et al. 2014). With these instrumental settings, the ^{180}Hf signal intensity of the reference material rutile R10 (Hf ~ 40 μg g^{-1}) was ca. 0.25 V. Corrections for isobaric interferences and mass bias were similar to those described in Ewing et al. (2011) and Li et al. (2015a). The isobaric interferences of ^{176}Yb and ^{176}Lu on ^{176}Hf were calculated from the measured ^{173}Yb and ^{175}Lu intensities and natural ratios of $^{176}Yb/^{173}Yb$ (0.79381; Segal et al. 2003) and $^{176}Lu/^{175}Lu$ (0.02656; Wu et al. 2006). The very low Yb content in rutile makes it difficult to determine an accurate mass bias factor for Yb using the measured $^{173}Yb/^{171}Yb$, as is often conducted in zircon Hf isotopic measurements. Therefore, the mass bias factors for Yb and Lu were assumed to be the same as that for Hf. The very low Yb and Lu contents make $^{176}Hf/^{177}Hf$ insensitive to the mass bias factors for Yb and Lu (Li et al. 2015a). Instrumental mass bias for Hf was corrected based on the measured $^{179}Hf/^{177}Hf$ and its natural ratio (0.7325; Blichert-Toft et al. 1997), using an exponential law. Forty-five analyses of R10 yielded a mean $^{176}Hf/^{177}Hf$ value of 0.282169 ± 0.000211 (2s), in agreement with the results reported by Luvizotto et al. (2009) and Li et al. (2015a) (0.282178 ± 0.000012 and 0.282157 ± 0.000204, respectively). Thirty analyses of the Penglai zircon reference material yielded a mean $^{176}Hf/^{177}Hf$ value of 0.282915 ± 0.000037 (2s), in agreement with the recommended value (0.282906 ± 0.000010) reported by Li et al. (2010).

Results and discussion

High-resolution X-ray elemental mapping

Forty-two RMJG rutile grains were tested for core-rim chemical homogeneity by X-ray mapping. From core to rim, each RMJG crystal showed nearly homogeneous V, Cr, Zr, Nb, Hf and U contents (Figure 3). The mass fraction occasionally varied between different rutile grains. For example, one rutile shown in Figure 3d has an obviously different Cr content from the other grains, and two rutiles shown in Figure 3e have different Zr contents from the others. Therefore, the RMJG rutile is not a suitable reference material for trace element determination.

Trace element mass fractions

One hundred and seven trace element determinations of the RMJG rutiles are summarised in Table S2. Each analysis was performed on a different rutile grain. The most homogeneous trace element in RMJG rutiles is U, which showed a variation within ± 17%. Vanadium, Zn and Nb displayed slightly larger variations (two relative standard deviations [2 RSD] = 23–26%) than U. The variations of Sc, Cr and Hf were around 35% (2 RSD). More than 85% of the measured rutile grains had > 80 μg g^{-1} Hf, and showed much less variation (2 RSD = 12%). Thorium contents varied from 0.01 μg g^{-1} to below detection limits, and most crystals have Th < 0.002 μg g^{-1}. Ytterbium and Lu contents were also very low (< 0.03 and < 0.01 μg g^{-1}, respectively) and, for most crystals, below detection limits. Compared with other rutile reference materials (e.g., R10 and R19, Zack et al. 2011; Sugluk-4 and PCA-S207, Bracciali et al. 2013), the RMJG rutile has higher Hf (~ 102 μg g^{-1}) and U (~ 60 μg g^{-1}) contents. The total radiogenic Pb (^{206}Pb and ^{207}Pb) calculated based on the U contents (50.1– 80.4 μg g^{-1}) and U-Pb age (1750 Ma), is 16–24 μg g^{-1}. The Zr content varied from 702 to 3122 μg g^{-1}, with a mean of 2537 ± 1078 (2s) μg g^{-1}. Zr-Hf and Nb-Ta contents display broad positive correlations (Figure 4). According to the Zr-in-rutile geothermometer proposed by Tomkins et al. (2007), the RMJG rutiles formed at 857 ± 69 °C, assuming a pressure of 10 kbar. The RMJG rutiles have Zr/Hf, Nb/Ta and Nb/Cr ratios of 24.5 ± 4.8, 24.0 ± 8.7 and 0.31 ± 0.14, respectively, consistent with rutiles from metapelites according to the discrimination diagram presented in Triebold et al. (2007).

U-Pb dating

ID-TIMS: Eight sub-samples of the RMJG rutile were analysed by ID-TIMS, and all plot on the concordia line,
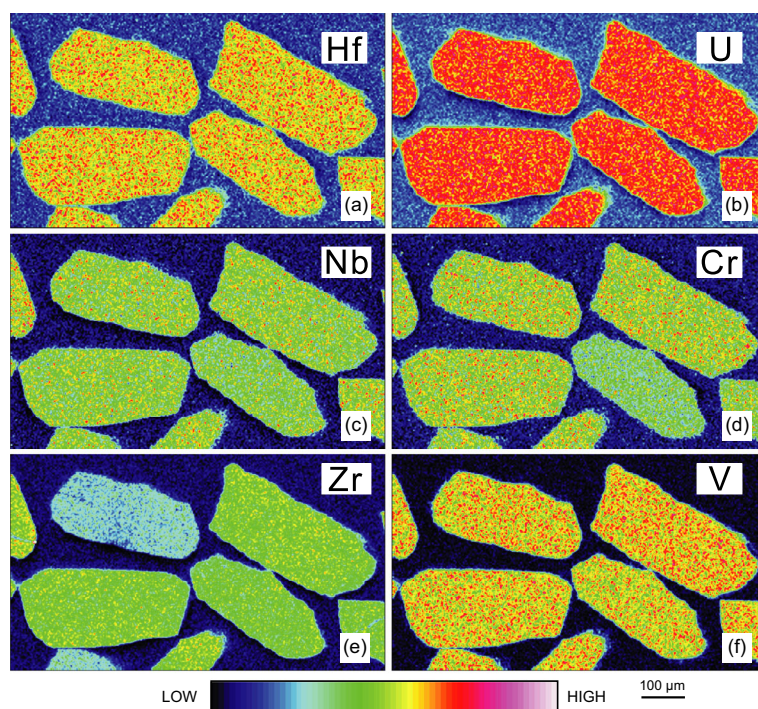
Figure 3. X-ray elemental maps of typical RMJG rutile grains for (a) Hf, (b) U, (c) Nb, (d) Cr, (e) Zr and (f) V. [Colour figure can be viewed at wileyonlinelibrary.com]
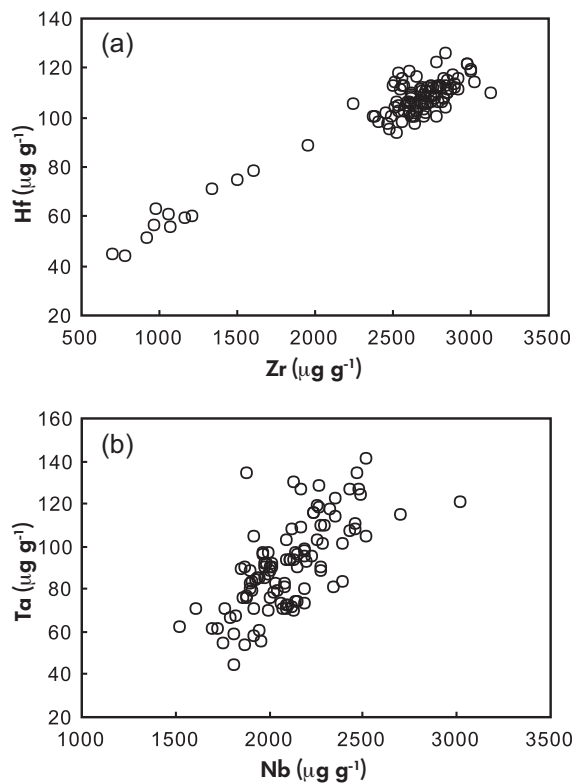

Figure 4. Plots of (a) Hf-Zr and (b) Ta-Nb for the RMJG rutile. Measured with LA-SF-ICP-MS. Each point represents an individual rutile grains.
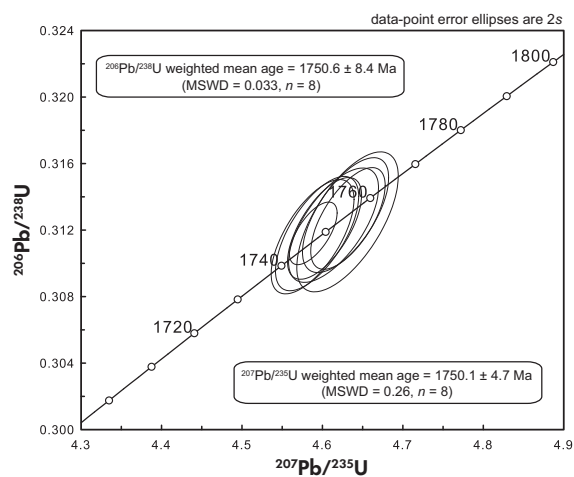

Figure 5. Concordia plot for ID-TIMS data of the RMJG rutile. Error ellipses represent 2s.

yielding a weighted mean $^{207}Pb/^{206}Pb$ age of 1751.5 ± 4.3 Ma, a $^{206}Pb/^{238}U$ age of 1750.6 ± 8.4 Ma and a $^{207}Pb/^{235}U$ age of 1750.1 ± 4.7 Ma (Figure 5; Table 1). Therefore, 1750.6 ± 8.4 Ma is our best estimate for the age of the RMJG rutile. The U content measured by ID-TIMS is 50.8 ± 34.1 µg g^{-1}, which is consistent with the LA-ICP-MS analyses.

Table 1.
U-Pb dating results for the RMJG rutile obtained by ID-TIMS

No.	Mass (g)	Pb ($\mu g\ g^{-1}$)	U ($\mu g\ g^{-1}$)	$^{206}Pb/$ ^{208}Pb [a]	Radiogenic isotope ratio						Ages (Ma)					
					$^{207}Pb/$ ^{235}U	2s	$^{206}Pb/$ ^{238}U	2s	$^{207}Pb/$ ^{206}Pb	2s	$^{207}Pb/$ ^{235}U	2s	$^{206}Pb/$ ^{238}U	2s	$^{207}Pb/$ ^{206}Pb	2s
1	0.0015	13.7	46	945	4.6312	0.038	0.3126	0.0025	0.1074	0.00011	1754.9	13.6	1753.5	24.8	1755.8	3.7
2	0.00265	8.7	29	5412	4.6136	0.046	0.3122	0.0028	0.1072	0.00038	1751.7	16.4	1751.5	27.9	1752.4	12.8
3	0.00174	10.1	34	2986	4.5882	0.024	0.3117	0.0016	0.1068	0.00015	1747.1	8.8	1749.1	15.3	1745.5	5.1
4	0.00147	14.9	50	1456	4.6021	0.038	0.312	0.0025	0.107	0.00013	1749.6	13.6	1750.5	24.8	1748.9	4.4
5	0.00224	15.2	51	9568	4.6283	0.044	0.3128	0.0028	0.1073	0.00028	1754.4	15.7	1754.5	27.9	1754.1	9.5
6	0.00207	16.7	56	1546	4.6306	0.052	0.3124	0.0035	0.1075	0.00010	1754.8	18.5	1752.5	34.0	1757.5	3.3
7	0.00114	25.4	85	10521	4.593	0.042	0.3117	0.0028	0.1069	0.00011	1748.0	15.2	1749.1	27.8	1747.2	3.7
8	0.00143	16.4	55	2198	4.5872	0.042	0.3115	0.0028	0.1068	0.00015	1746.9	15.2	1748.1	27.8	1745.5	5.1

Uncertainties are 2s. $^{207}Pb/^{235}U$ ratios calculated using $^{238}U/^{235}U$ = 137.818. Age calculations use the decay constants of Jaffey et al. (1971). No correction for initial disequilibrium in $^{230}Th/^{238}U$ was performed for $^{206}Pb/^{238}U$ and $^{207}Pb/^{206}Pb$ ages. All grains were soaked in ultrapure anhydrous alcohol, 7 mol l^{-1} HNO$_3$ and 2 mol l^{-1} HCl for 3, 4 and 12 h, respectively. No air abrading was used. Total procedural blank was 50 pg for Pb and was corrected based on the blank Pb isotopic composition ($^{206}Pb/^{204}Pb$ = 17.83, $^{207}Pb/^{204}Pb$ = 15.47, $^{208}Pb/^{204}Pb$ = 37.41).
[a] Measured $^{206}Pb/^{208}Pb$ corrected for fractionation and spike.

LA-ICP-MS: The U-Pb ages of the RMJG rutile determined by LA-(MC/SF)-ICP-MS are listed in Table S3. Three sessions of LA-MC-ICP-MS analyses comprising a total of 160 U-Pb age determinations on 155 rutiles, two sessions of LA-SF-ICP-MS analyses comprising a total of ninety-six U-Pb age determinations on ninety-four rutiles, and three sessions of LA-ICP-MS analyses comprising a total of 135 U-Pb age determinations on 133 rutiles were conducted in two different laboratories over 5 months. The three sessions of LA-MC-ICP-MS U-Pb isotopic determinations yielded weighted mean $^{206}Pb/^{238}U$ and $^{207}Pb/^{235}U$ ages of 1749.8 ± 2.2 Ma and 1749.8 ± 1.9, respectively (Figure 6a). The two sessions of LA-SF-ICP-MS U-Pb isotopic determinations yielded weighted mean $^{206}Pb/^{238}U$ and $^{207}Pb/^{235}U$ ages of 1749.2 ± 3.2 Ma and 1749.3 ± 2.9, respectively (Figure 6b). The three sessions of LA-ICP-MS U-Pb isotopic determinations yielded weighted mean $^{206}Pb/^{238}U$ and $^{207}Pb/^{235}U$ of 1749.2 ± 3.5 Ma and 1749.9 ± 2.3 Ma, respectively (Figure 6c). The U-Pb ages obtained from both laboratories are identical within analytical uncertainties. All the 391 in situ measurements (LA-MC-ICP-MS, LA-SF-ICP-MS and LA-ICP-MS) define Gaussian distributions for $^{207}Pb/^{206}Pb$, $^{206}Pb/^{238}U$ and $^{207}Pb/^{235}U$ ages, with a mean $^{207}Pb/^{206}Pb$ age of 1751.9 ± 47.7 Ma (2s), $^{206}Pb/^{238}U$ age of 1749.9 ± 32.1 Ma (2s) and $^{207}Pb/^{235}U$ age of 1750.0 ± 26.4 Ma (2s) (Figure 7), which are statistically indistinguishable from the ID-TIMS age. Previous studies indicated that Pb volume diffusion behaviour in rutile is size-dependent (e.g., Mezger et al. 1989, Cherniak 2000, Smye et al. 2018). To demonstrate whether RMJG rutiles had experienced significant Pb volume diffusion, we measured the width of all the RMJG rutile grains analysed with LA-ICP-

MS (Table S3). With the change of the width of rutile grains, little systematic variation of the measured $^{206}Pb/^{238}U$ age was observed (Figure S2). In addition, three RMJG rutile grains were selected to perform age profile measurement. From core to rim, the measured $^{206}Pb/^{238}U$ ages were relatively constant within analytical error (Figure S3). As such, the RMJG rutiles define a homogeneous U-Pb age, even at the scale of an individual crystal. The U-Pb age of RMJG rutile (1750 Ma) is much less than the U-Pb of zircons (> 1840 Ma) in the same host pelitic granulite. This is because rutile has a much lower closure temperature (~ 500 °C) than zircon (~ 900 °C) and the U-Pb system of RMJG rutile was reset by later thermal events. Mafic dyke swarms with an age range of 1730–1780 Ma occur in the study area (Peng et al. 2008, Peng 2015, Li et al. 2015b). Therefore, it is likely that these dyke swarms were emplaced into shallow crust and heated the rutiles. As the temperature was higher than the closure temperature, the U-Pb system in rutiles was reset. More work is needed to discuss the geological meaning of the rutile U-Pb age.

Hf isotopic composition

Four sub-samples of the RMJG rutile were digested and analysed for their Hf isotopic composition by MC-ICP-MS in solution mode. Three duplicate analyses were conducted on each sample solution. The measured $^{176}Hf/^{177}Hf$ of all twelve analyses in solution mode yielded a mean value of 0.281652 ± 0.000007 (2s; Figure 8). The 238 analyses of 235 rutiles by LA-MC-ICP-MS were conducted in five different measurement sessions over 6 months. The mean $^{176}Hf/^{177}Hf$ values of the sessions are as follows: 0.28169 ± 0.00019 (2s, n = 40), 0.28160 ± 0.00017
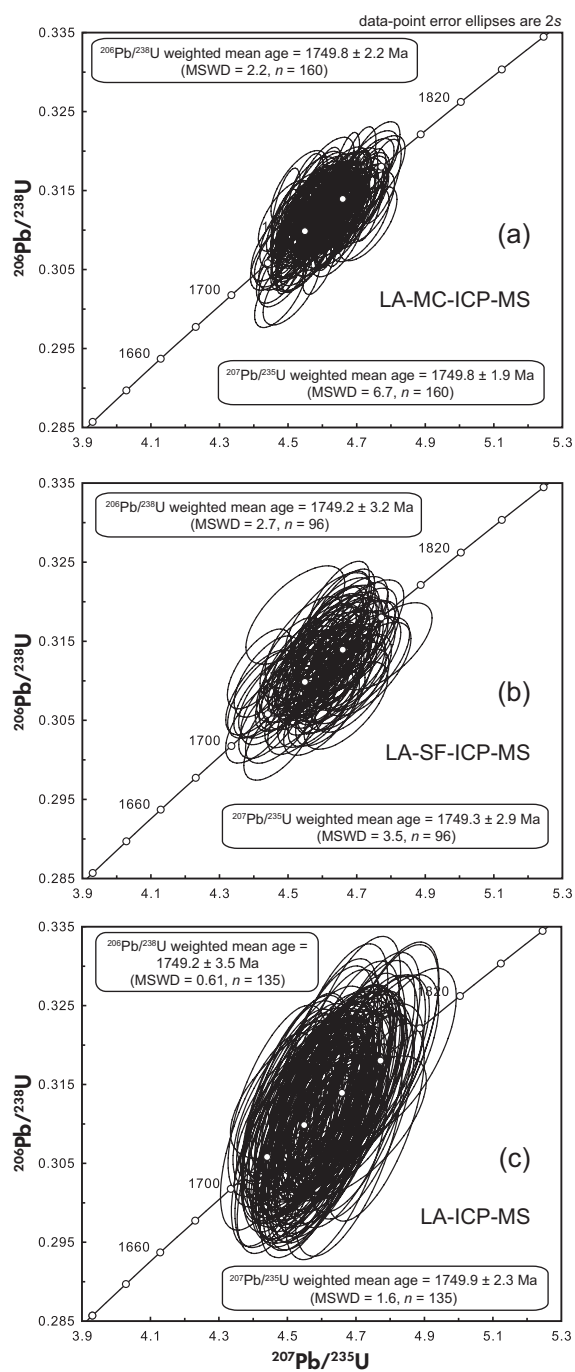
Figure 6. Concordia plots of the RMJG rutile measured with (a) LA-MC-ICP-MS, (b) LA-SF-ICP-MS and (c) LA-ICP-MS. Laser conditions: beam size of 24 μm, repetition rate of 5 Hz, energy density of 4 J cm^{-2} for LA-MC-ICP-MS; beam size of 33 μm, repetition rate of 5 Hz, energy density of 4 J cm^{-2} for LA-SF-ICP-MS; beam size of 32 μm, repetition rate of 5 Hz, energy density of 5 J cm^{-2} for LA-ICP-MS. All ellipses represent 2s.
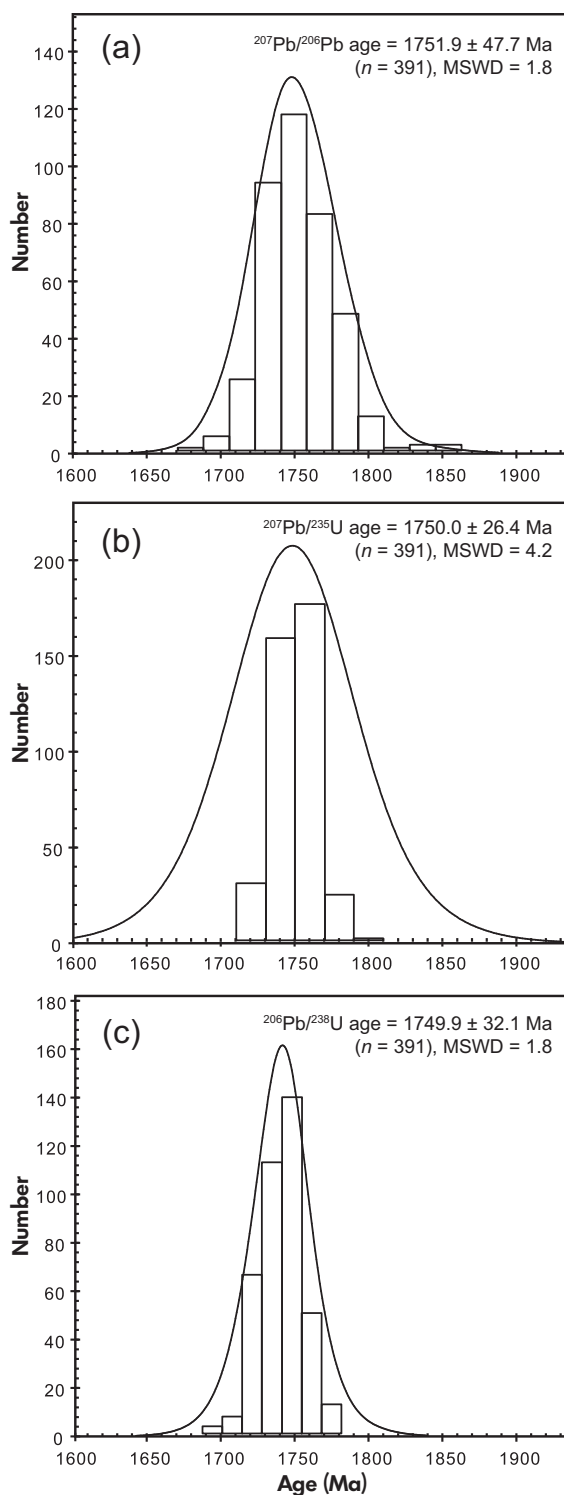

Figure 7. Histograms of (a) ^{207}Pb/^{206}Pb, (b) ^{207}Pb/^{235}U and (c) ^{206}Pb/^{238}U ages for all the laser ablation U-Pb isotopic data.
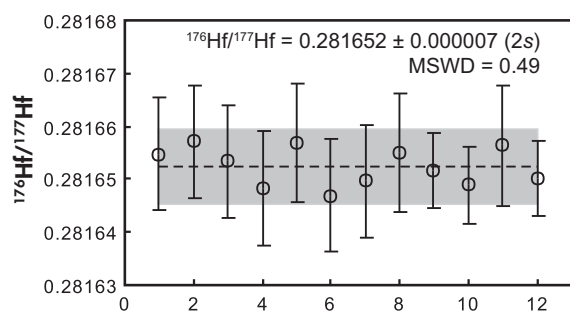
Figure 8. $^{176}Hf/^{177}Hf$ ratios of the RMJG rutile measured by solution MC-ICP-MS. Twelve sets of analyses gave a $^{176}Hf/^{177}Hf$ value of 0.281652 ± 0.000007 (2*s*). Error bars are 2SE.

(2*s*, *n* = 32), 0.28167 ± 0.00017 (2*s*, *n* = 56), 0.28164 ± 0.00014 (2*s*, *n* = 47) and 0.28165 ± 0.00015 (2*s*, *n* = 63) (Figure 9; Table S4). All 238 analyses define a Gaussian distribution for $^{176}Hf/^{177}Hf$ and yielded a mean $^{176}Hf/^{177}Hf$ value of 0.28166 ± 0.00018 (2*s*; Figure 10), suggesting the rutiles have a homogenous Hf isotopic composition.

Summary of rutile reference materials

Recently, several natural rutiles have been proposed as reference materials for microbeam U-Pb age determination and the Hf isotopic homogeneity of some of these rutiles has been tested (Table 2). The ages of these reference rutiles are from the Neo-Archaean to late Cambrian (2642–490 Ma). R10, R19 and JDX are centimetre-scale single crystals with relatively homogeneous trace element mass fractions,
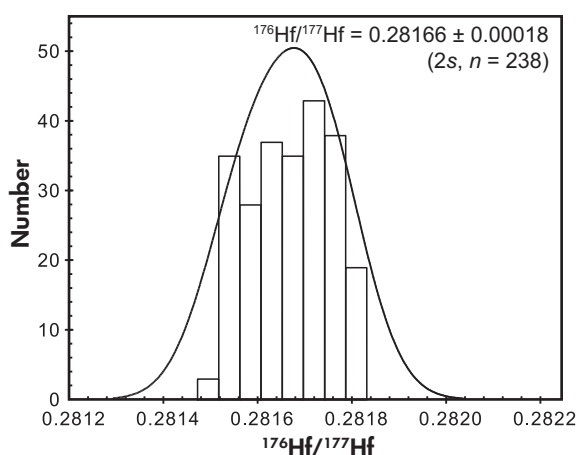

Figure 10. Histogram of $^{176}Hf/^{177}Hf$ ratios for the RMJG rutile measured by LA-MC-ICP-MS.

whereas other rutiles are much smaller (around several hundred micrometres) with relatively large variations of trace elements. This means R10, R19 and JDX are potential trace elemental reference materials. However, because they are single crystals, the distribution of these three rutiles may be limited. Compared with JDX and R19, except PCA-S207 with high common Pb, other rutiles with high U and radiogenic Pb are more suitable for microbeam U-Pb determination.

At this stage, only RMJG, R10, JDX and R19 have been analysed for Hf isotope determination by the solution MC-ICP-MS method. Using LA-MC-ICP-MS, Li *et al.* (2015a) measured Hf isotopes in PCA-S207 and Sugluk-4. All these measured rutiles display homogeneous Hf isotopic ratios
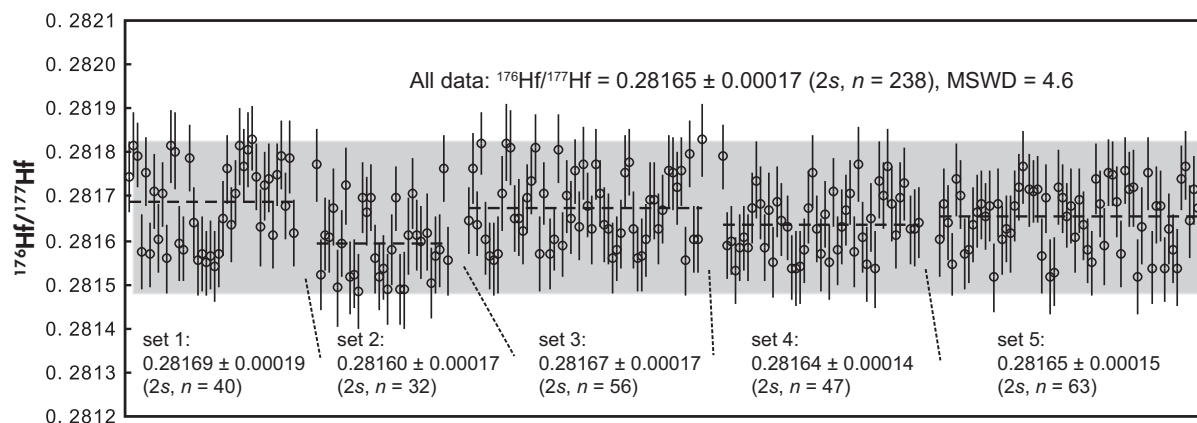

Figure 9. $^{176}Hf/^{177}Hf$ ratios of the RMJG rutile measured by LA-MC-ICP-MS. Two-hundred and eight analyses yielded a mean $^{176}Hf/^{177}Hf$ value of 0.28166 ± 0.00018 (2*s*), identical with the value measured with solution MC-ICP-MS within analytical error. Laser condition: beam size of 155 μm, repetition rate of 8 Hz and energy density of 4 J cm^{-2}. Error bars are 1SE.

Table 2.
Summary of natural rutile reference materials used/proposed for U-Pb and Hf isotope microanalyses

RM	Age (Ma)	U (µg g⁻¹)	Th (µg g⁻¹)	Pb_{rad} (µg g⁻¹) [a]	Pb_{com}% [b]	Hf (µg g⁻¹)	$^{176}Hf/^{176}Hf$	Grain size	Rock	Ref. for age	Ref. for Hf isotopes
WH-1/JIMP-1B	2642	~ 100		~ 50	< 0.2%	36.9 ± 27	0.281246 (146) [c]	Coarse-grained quartzite		1, 2	
PCA-S207	1865	22.8 ± 19	0.0006 ± 0.004	7.8 ± 2.7	2.9–45%	102 ± 34	0.281652 (6)	0.1–0.5 mm	Garnet-bearing paragneiss	3	4
RMG	1750	80.4 ± 10.6		17.9 ± 3.2	< 0.5%	51.3 ± 19	0.281172 (107) [c]	0.1–0.5 mm	Pelitic granulite	This study	This study
Sugluk-4	1719	59.5 ± 60.6		16.4 ± 21	0.2–1.6%			0.1–0.5 mm	Granulite facies quartzite	3	4
R10, R10b	1091	44.1 ± 1.2	< 0.00035	7.5	0.2–1.6%	37.2 ± 0.2	0.282178 (12)	cm scale single crystal	Amphibolite-facies metamorphic rock	5	5
JDX	510	~ 6		~ 0.45		50.1 ± 0.7	0.281795 (15)	Single crystal 5 cm	Unclear	6	4
R632	496	153–1000	0.2–5	11–72	0.1–2.4%	108 ± 11		0.1–1 mm	Sakenite	7	
R19	490	14.4 ± 0.8	0.012 ± 0.01	1		8.1 ± 0.4	0.282163 (17)	cm scale single crystal	Unclear	1	5

References: 1 Zack et al. (2011); 2 Schmitt and Zack (2012) CG; 3 Bracciali et al (2013); 4 Li et al (2015a); 5 Luvizotto et al (2009); 6 Li et al. (2011); 7 Axelsson et al. (2018).
[a] Radiogenic Pb contents calculated from their ages and U contents.
[b] Common Pb proportion.
[c] Measured with LA-MC-ICP-MS; Hf isotopes for other samples measured with solution MC-ICP-MS.

when the analytical error is considered. Among these rutiles, R19 has the lowest Hf mass fraction, whereas RMJG and R632 have the highest. However, the homogeneity of Hf isotopic ratio in R632 has not been tested. Therefore, considering the Hf mass fraction, RMJG is now the most suitable reference material for Hf isotopic microanalysis.

Conclusions

ID-TIMS, LA-MC-ICP-MS, LA-SF-ICP-MS and LA-ICP-MS analyses demonstrate that the RMJG rutile is homogeneous with respect to its U-Pb age and Hf isotopic composition at the ~ 30 and ~ 150 µm scale, respectively. The microbeam U-Pb dating results are identical within analytical error to the ID-TIMS age. Precise measurement of the $^{176}Hf/^{177}Hf$ value by solution MC-ICP-MS is identical to the mean LA-MC-ICP-MS measurement. The recommended U-Pb age and $^{176}Hf/^{177}Hf$ value of the RMJG rutile are 1750.6 ± 8.4 Ma and 0.281652 ± 0.000007 (2s), respectively. The RMJG rutile is available as a mineral separate in batches of about 5–10 mg each from the authors.

Acknowledgements

Data availability statement

All data used in this study are supplied as electronic supporting materials.

References

Axelsson E., Pape J., Berndt J., Corfu F., Mezger K. and Raith M.M. (2018)
Rutile R632 – A new natural reference material for U-Pb and Zr determination. Geostandards and Geoanalytical Research, 42, 319–338.

Blichert-Toft J., Chauvel C. and Albarède F. (1997)
Separation of Hf and Lu for high-precision isotope analysis of rock samples by magnetic sector-multiple collector ICP-MS. Contributions to Mineralogy and Petrology, 127, 248–260.

Bracciali L., Parrish R.R., Horstwood M.S.A., Condon D.J. and Najman Y. (2013)
U-Pb LA-(MC)-ICP-MS dating of rutile: New reference materials and applications to sedimentary provenance. Chemical Geology, 347, 82–101.

Cherniak D.J. (2000)
Pb diffusion in rutile. Contribution to Mineralogy and Petrology, 139, 198–207.

Ewing T.A., Rubatto D., Eggins S.M. and Hermann J. (2011)
In situ measurement of hafnium isotopes in rutile by LA-MC-ICP-MS: Protocol and applications. Chemical Geology, 281, 72–82.

Ewing T.A., Hermann J. and Rubatto D. (2013)
The robustness of the Zr-in-rutile and Ti-in-zircon thermometers during high-temperature metamorphism (Ivrea-Verbano Zone, northern Italy). Contributions to Mineralogy and Petrology, 165, 757–779.

Ewing T.A., Rubatto D. and Hermann J. (2014)
Hafnium isotopes and Zr/Hf of rutile and zircon from lower crustal metapelites (Ivrea-Verbano Zone, Italy): Implications for chemical differentiation of the crust. Earth and Planetary Science Letters, 389, 106–118.

Hu Z., Liu Y., Gao S., Liu W., Zhang W., Tong X., Lin L., Zong K., Li M., Chen H., Zhou L. and Yang L. (2012)
Improved in situ Hf isotope ratio analysis of zircon using newly designed X skimmer cone and jet sample cone in combination with the addition of nitrogen by laser ablation multiple collector ICP-MS. Journal of Analytical Atomic Spectrometry, 27, 1391–1399.

Jaffey A.H., Flynn K.F., Glendenin L.E., Bentley W.T. and Essling A.M. (1971)
Precision measurement of half-lives and specific activities of 235U and 238U. Physical Review C, 4, 1889–1906.

Kimura J.-I. and Chang Q. (2012)
Origin of the suppressed matrix effect for improved analytical performance in determination of major and trace elements in anhydrous silicate samples using 200 nm femtosecond laser ablation sector-field inductively coupled plasma-mass spectrometry. Journal of Analytical Atomic Spectrometry, 27, 1549–1559.

Kooijman E., Mezger K. and Berndt J. (2010)
Constraints on the U-Pb systematics of metamorphic rutile from in situ LA-ICP-MS analysis. Earth and Planetary Science Letters, 293, 321–330.

Li X.H., Long W.G., Li Q.L., Liu Y., Zheng Y.F., Yang Y.H., Chamberlain K.R., Wan D.F., Guo C.H. and Wang X.C. (2010)
Penglai zircon megacrysts: A potential new working reference material for microbeam determination of Hf-O isotopes and U-Pb age. Geostandards and Geoanalytical Research, 34, 117–134.

references

Li Q., Lin W., Su W., Li X.-H., Shi Y.-H., Liu Y. and Tang G.-Q. (2011)
SIMS U-Pb rutile age of low-temperature eclogites from southwestern Chinese Tianshan, NW China. **Lithos, 122,** 76–86.

Li Y., Yang Y., Jiao S., Wu F., Yang J., Xie L. and Huang C. (2015a)
In situ determination of hafnium isotopes from rutile using LA-MC-ICP-MS. **Science China Earth Sciences, 58,** 2134–2144.

Li Y., Peng P., Wang X. and Wang H. (2015b)
Nature of 1800–1600 Ma mafic dyke swarms in the North China Craton: Implications for the rejuvenation of the sub-continental lithospheric mantle. **Precambrian Research, 257,** 114–123.

Ludwig K.R. (1988)
PBDAT for MS–DOS.A computer program for IBM-PC compatibles for processing raw Pb-U-Th isotope data, version 1.00a. **United States Geological Survey Open File Report, 88–542,** 37pp.

Ludwig K.R. (2005)
User's Manual for ISOPLOT/Ex 3.22. A geochronological toolkit for Microsoft Excel. **Berkeley Geochronology Center Special Publication,** 1–71.

Luvizotto G.L, Zack T., Meyer H.P., Ludwig T., Triebold S., Kronz A., Münker C., Stöckli D.F., Prowatke S., Klemme S., Jacob D.E. and von Eynatten H. (2009)
Rutile crystals as potential trace element and isotope mineral standards for microanalysis. **Chemical Geology, 261,** 346–369.

Meinhold G. (2010)
Rutile and its applications in earth sciences. **Earth-Science Reviews, 102,** 1–28.

Meinhold G., Anders B., Kostopoulos D. and Reischmann T. (2008)
Rutile chemistry and thermometry as provenance indicator: An example from Chios Island, Greece. **Sedimentary Geology, 203,** 98–111.

Mezger K., Hanson G.N. and Bohlen S.R. (1989)
High-precision U-Pb ages of metamorphic rutiles: Application to the cooling history of high-grade terranes. **Earth and Planetary Science Letters, 96,** 106–118.

Mezger K., Rawnsley C.M., Bohlen S.R. and Hanson G.N. (1991)
U-Pb garnet, sphene, monazite, and rutile ages: Implications for the duration of high-grade metamorphism and cooling histories, Adirondack Mts., New York. **The Journal of Geology, 99,** 415–428.

Pape J., Mezger K. and Robyr M. (2016)
A systematic evaluation of the Zr-in-rutile thermometer in ultra-high temperature (UHT) rocks. **Contributions to Mineralogy and Petrology, 171,** 44.

Peng P. (2015)
Precambrian mafic dyke swarms in the North China Craton and their geological implications. **Science China Earth Sciences, 58,** 649–675.

Peng P., Zhai M., Ernst R.E., Guo J., Liu F. and Hu B. (2008)
A 1.78 Ga large igneous province in the North China craton: The Xiong'er Volcanic Province and the North China dyke swarm. **Lithos, 101,** 260–280.

Schmitt A. and Zack T. (2012)
High-sensitivity U-Pb rutile dating by secondary ion mass spectrometry (SIMS) with an O^{2+} primary beam. **Chemical Geology, 332–333,** 65–73.

Segal I., Halicz L. and Platzner I.T. (2003)
Accurate isotope ratio measurements of ytterbium by multiple collection inductively coupled plasma-mass spectrometry applying erbium and hafnium in an improved double external normalization procedure. **Journal of Analytical Atomic Spectrometry, 18,** 1217–1223.

Smye A., Marsh J., Vermeesch P., Garber J. and Stöckli D. (2018)
Applications and limitations of U-Pb thermochronology to middle and lower crustal thermal histories. **Chemical Geology, 494,** 1–18.

Stacey J.S. and Kramers J.D. (1975)
Approximation of terrestrial lead isotope evolution by a two-stage model. **Earth and Planetary Science Letters, 26,** 207–221.

Stendal H., Toteu S.F., Frei R., Penaye J., Njel U.O., Bassahak J., Nni J., Kankeu B., Ngako V. and Hell J.V. (2006)
Derivation of detrital rutile in the Yaoundé region from the Neoproterozoic Pan-African belt in southern Cameroon (Central Africa). **Journal of African Earth Sciences, 44,** 443–458.

Tomkins H.S., Powell R. and Ellis D.J. (2007)
The pressure dependence of the zirconium-in-rutile thermometer. **Journal of Metamorphic Geology, 25,** 703–713.

Triebold S., von Eynatten H., Luvizotto G.L. and Zack T. (2007)
Deducing source rock lithology from detrital rutile geochemistry: An example from the Erzgebirge, Germany. **Chemical Geology, 244,** 421–436.

Triebold S., von Eynatten H. and Zack T. (2012)
A recipe for the use of rutile in sedimentary provenance analysis. **Sedimentary Geology, 282,** 268–275.

Tu J.-R., Cui Y.-R., Hao S., Li H.-M., Zhou H.-Y. and Geng J.-Z. (2016)
An investigation of U-Pb isotope dating of cassiterite with isotope dilution-thermal ionization mass spectrometry. **Acta Geoscientia Sinica, 37,** 779–783. (in Chinese with English abstract)

Watson E.B., Wark D.A. and Thomas J.B. (2006)
Crystallization thermometers for zircon and rutile. **Contributions to Mineralogy and Petrology, 151,** 413.

Wu F.-Y., Yang Y.-H., Xie L.-W., Yang J.-H. and Xu P. (2006)
Hf isotopic compositions of the standard zircons and baddeleyites used in U-Pb geochronology. **Chemical Geology, 234,** 105–126.

references

Wu J.-L., Zhang H.-F., Zhai M.-G., Guo J.-H., Liu L, Yang W.-Q., Wang H.-Z., Zhao L, Jia X.-L. and Wang W. (2016)
Discovery of pelitic high-pressure granulite from Manjing-gou of the Huai'an Complex, North China Craton: Metamorphic P-T evolution and geological implications. Precambrian Research, 278, 323–336.

Wu J., Zhai M., Zhang H. and Hu B. (2018)
An analysis of mineralogical characteristics and metamorphism of Palaeoproterozoic pelitic granulites from Datong-Huai'an area, the North China Craton. Acta Petrologica Sinica, 34, 3266–3286. (in Chinese with English abstract)

Wu J., Zhang H., Zhai M., Zhang H., Wang H., Li R., Hu B. and Zhang H. (2019)
Shared metamorphic histories of various Palaeoproterozoic granulites from Datong–Huai'an area, North China Craton (NCC): Constraints from zircon U-Pb ages and petrology. International Geology Review, 61, 694–719.

Xia X., Ren Z., Wei G., Zhang L, Sun M. and Wang Y. (2013)
In situ rutile U-Pb dating by laser ablation-MC-ICP-MS. Geochemical Journal, 47, 459–468.

Xing C.-M., Wang C.Y. and Tan W. (2017)
Disequilibrium growth of olivine in mafic magmas revealed by phosphorus zoning patterns of olivine from mafic–ultramafic intrusions. Earth and Planetary Science Letters, 479, 108–119.

Zack T. and Kooijman E. (2017)
Petrology and geochronology of rutile. Reviews in Mineralogy and Geochemistry, 83, 443–467.

Zack T. and Luvizottow G.L. (2006)
Application of rutile thermometry to eclogites. Mineralogy and Petrology, 88, 69–85.

Zack T., Moraes R. and Kronz A. (2004a)
Temperature dependence of Zr in rutile: Empirical calibration of a rutile thermometer. Contributions to Mineralogy and Petrology, 148, 471–488.

Zack T., von Eynatten H. and Kronz A. (2004b)
Rutile geochemistry and its potential use in quantitative provenance studies. Sedimentary Geology, 171, 37–58.

Zack T., Stöckli D.F., Luvizotto G.L., Barth M.G., Belousova E., Wolfe M.R. and Hinton R.W. (2011)
In situ U-Pb rutile dating by LA-ICP-MS: ^{208}Pb correction and prospects for geological applications. Contributions to Mineralogy and Petrology, 162, 515–530.

Zhai M., Guo J., Li Y., Liu W., Peng P. and Shi X. (2003)
Two linear granite belts in the central-western North China Craton and their implication for Late Neoarchaean-Palaeoproterozoic continental evolution. Precambrian Research, 127, 267–283.

Zhang L, Ren Z.-Y., Nichols A.R.L, Zhang Y.-H., Zhang Y., Qian S.-P. and Liu J.-Q. (2014)
Lead isotope analysis of melt inclusions by LA-MC-ICP-MS. Journal of Analytical Atomic Spectrometry, 29, 1393–1405.

Zhang L, Ren Z.-Y., Xia X.-P., Yang Q., Hong L.-B. and Wu D. (2019)
In situ determination of trace elements in melt inclusions using laser ablation inductively coupled plasma sector field mass spectrometry. Rapid Communications in Mass Spectrometry, 33, 361–370.

Zheng Y.-F., Gao X.-Y., Chen R.-X. and Gao T. (2011)
Zr-in-rutile thermometry of eclogite in the Dabie orogen: Constraints on rutile growth during continental subduction-zone metamorphism. Journal of Asian Earth Sciences, 40, 427–451.

Zhou H., Li H., Cui Y., Geng J., Zhang J. and Li H. (2013)
Rutile U-Pb isotopic dating methodology. Acta Geologica Sinica, 87, 1439–1446. (in Chinese with English abstract)

Supporting information

The following supporting information may be found in the online version of this article:

Figure S1. (a) Sample locality for the RMJG rutile. (b) Appearance of the Manjinggou pelitic granulite, which hosts the RMJG rutile.

Figure S2. LA-ICP-MS ^{206}Pb/^{238}U age of RMJG rutile grains vs the width of the rutile grains.

Figure S3. Age profiles of three RMJG rutile crystals measured by LA-MC-ICP-MS.

Table S1. Instrumental settings for U-Pb dating with LA-ICP-MS.

Table S2. Trace elements measured by LA-SF-ICP-MS.

Table S3. LA-ICP-MS U-Pb data.

Table S4. Hf isotope measured by LA-MC-ICP-MS.

This material is available from: http://onlinelibrary.wiley.com/doi/10.1111/ggr.12304/abstract (This link will take you to the article abstract).